

# Study on stability of landslide at different moisture content in northern slope of Bailu tableland

Han Guo <sup>1\*</sup>, Jichao Sun <sup>1</sup>, Mingzhi Liu <sup>1</sup>

<sup>1</sup>School of Water Resource & Environment, China University of Geosciences, Beijing, 100083, China

\* Corresponding author E-mail: Han Guo

**Abstract:** In this paper, Phase2 software is used to simulate six groups of natural loess specimens in the northern slope of Bailu Plateau landslide area. The effective steady-state shear strength of loess specimens under different moisture content (6%, 11%, 21%, 26%, 30%, 32%) is simulated. We analyzed the stress and displacement, and we used residual thrust method to calculate the stability of sliding surface at different moisture content. The stability of the northern slope of Bailu tableland is analyzed at different moisture content. The "9.17 northern slope landslide of Bailu tableland" is summarized. The comprehensive evaluation of the northern slope landslide of Bailu tableland is carried out, the paper analyzed treatment measures of landslide.

**Key words:** Landslide in northern slope of Bailu tableland; Residual thrust method; "9.17 landslide in northern slope of Bailu tableland"; Stability

## 1 Introduction

The landslide hazard is not as concentrated or violent as an earthquake, but the destruction is widespread, frequent and long-lasting. Sometimes it associated with earthquakes, the damage is enormous. In the past 20 years, the statistics show that major geological disasters that involving more than 100 people have occurred almost every year in China. Hong Kong is the earliest area to study the relationship between rainfall and landslides <sup>[1]</sup>. EW Braiid (1994) analyzed the rainfall data and landslides of Hong Kong from 1963 to 1982, they obtained that the critical rainfall intensity is 70 mm/d, they used 24-

hour process rainfall as the evaluation index to predict the possibility of landslide. Mark & Newman <sup>[2]</sup> (1990) analyzed the precipitation in January 1982 in a certain area of the United States. If the last monthly rainfall is  $\geq 300$  mm, the rainfall is  $\geq 250$  mm, that the landslide will occur on a large scale. Li Zhuofen (1997) <sup>[3]</sup> analyzed the relationship of landslide and rainstorm from the perspective of particle gradation, soil permeability and shear strength in Hong Kong, it is used to predict the stability of the slope. This study is the basis of domestic rainfall slope theory. Li Chang Jiang (2011) <sup>[4]</sup> established a pre-effective rainfall model based on the fractal statistics of landslide and related rainfall observations. It is determined that the rainfall attenuation coefficient is the standard for the variation of rainfall with observation time in the landslide process in the region. There are many geological disasters had achieved great results, they had prevented some landslide hazards. On January 29,2015, the landslide in Chen Jiacun, Hei Fangtai district Yong Jing county, Gan Su province was predicted timely. On April 29, 2015, the same district had predicted in Luo Jia landslide. More than 450 people were evacuated in time <sup>[5]</sup>. The research on landslide disasters and its stability evaluation have been nearly a hundred years old. Many experts and scholars have been working on landslide disasters for a long time. The literatures of landslide are thousands of articles every year. This paper discusses the causes of landslide in the northern area of Bailu tableland, in order to provide some reference for the prevention and control of landslide geological disasters.

## **2 Survey of the research area**

### **2.1 Geographical position**

Bailu tableland is located in the central Guan Zhong basin of Shaanxi. It is one of the districts of Xi'an in the east. There are many railways, the traffic is very convenient, it is one of the main freight stations in Xi'an.

### **2.2 Topography and landform**

The northern slope of Bailu tableland is located in Shi Jiadao village, Xi Wang street, Ba Qiao district, Xi'an. It is located on the edge of the Loess tableland and closed to the west bank of Ba river. Bailu tableland has loess characteristics, it's scoured by runoff. Bailu

tableland was cut and denuded strongly, forming many parallel gullies. The gullies are 200~300 m apart. The mountain between the gullies is usually isolated and prominent. The topography is relatively gentle in the upper part and steep in others, the slope toe is slower [6] (Fig. 1).



**Figure 1** Landslide and landform (Satellite map) [According to Sun Weiqing, 2013]

### 2.3 Lithology

According to the field geological survey and combined with the collected data, it is mainly quaternary eolian and alluvial strata. The tertiary Miocene ( $N_1$ ) and Oligocene ( $E_3$ ) are mostly covered by the Quaternary, the bedrock is exposed in isolated places [7-8]. The exposed layer of Bailu tableland is mainly Quaternary loess with paleosol in the middle (Table 1).

**Table 1** Lithology of Quaternary strata at the edge of the landslide

Series	Symbol	Thickness/m	Properties
Holocene	Q <sub>4</sub> <sup>dl</sup>	1-5	The genetic is complicated, it's mainly slope deposits, and composed of loess-like soil and mélange, there is part of cultivated soil.
Upper Pleistocene	Q <sub>3</sub> <sup>eol</sup>	5-10	The loess is Gray-yellow to dark gray with large pore. It is no bedding. There are 1-2 layers of paleosol, near the surface is dark loessic soil. It is widely distributed in the loess tableland, and it belongs to eolian type.
Middle Pleistocene	Q <sub>2</sub> <sup>eol</sup>	15-45	The upper part are the coarse-grained loess with intercalation paleosol and a buried differentiation layer, the thickness is less than 25 m. The lower part are brown loess with four layers of intercalation paleosol and a buried differentiation layer, the thickness is less than 20 m.
Lower Pleistocene	Q <sub>1</sub> <sup>eol</sup>	26-45	It is Brownish yellow or light brown loess with intercalation degraded paleosol. The multilayer is 12-90 m thick. It belongs to eolian type.

## 2.4 Geological structure

The fault structure of the landslide developed in the east-west, north-east and north-west. It often causes geological disasters. The east-west buried active faults are mostly pre-Mesozoic basement faults. The other faults surface can extend to the Paleogene (Fig. 2). The fold structure in the area is not developed [9].

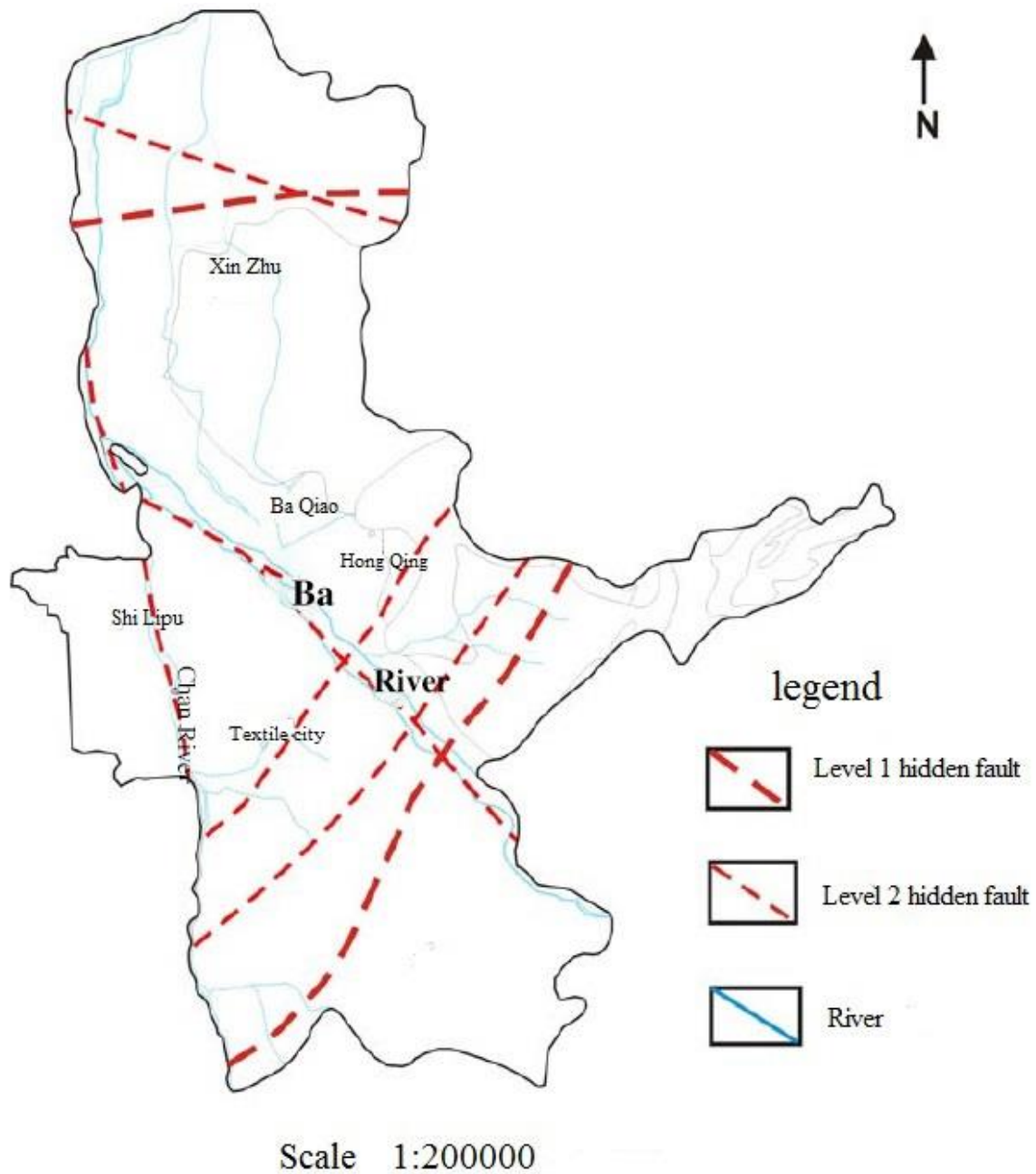


**Figure 2** Regional structural distribution map of Baqiao district

## 2.5 Hydrometeorology

Ba river flows through the north slope of Bailu tableland. The average annual runoff is 607 million cubic meters, it accounted for 33.6% from July to September, it is less from January to March and only 12.6%. According to the information of the Ma Duwang

hydrological station, the annual average sediment transport volume is 2,946,800 tons, the maximum is 9.36 million tons. The maximum sediment in the flood season is 955kg/m<sup>3</sup> (July 22, 1973). The maximum peak flow rate is 2166 m<sup>3</sup>/s (1957), and the minimum peak flow is 229 m<sup>3</sup>/s (1966). In the lower-precipitation years, the middle and lower reaches are often cut off [10]. The tableland is affected seriously by the erosion of the river, many stratum of Bailu tableland are exposed. The rainfall is increasing from northwest to southeast, the average annual precipitation is 584.9 mm. It is rainless and dry in winter. it is moderate in spring. Precipitation is concentrated from July to September The average annual precipitation is 97 days, the maximum is 138 days and the minimum is 74 days.

### **3 Calculation and analysis of stability theory formula at different moisture content in the north slope of Bailu tableland**

#### **3.1 Qualitative analysis of landslide**

The landslide of the northern slope of Bailu tableland has developed deformation locally, the external factors have gradually increased load crack development. The landslide is investigated from the scope, scale, failure mode and existing deformation signs. The stability of Bailu tableland is analyzed and evaluated qualitatively. The frontal zone of slope is cut to build factories and the loess is used to make bricks. It increases the gradient of the slope. The high-steep air surface provides a good dynamic foundation and caving space for the formation of the landslide. The slope is trapezoidal when viewed from above. the foot of the slope is wide about 200 m, the longitudinal length is 56 m, and the distribution elevation is 852 m. The shape of the slope is irregular, it is steep above and slow below, and the slope is nearly 70°. A small amount of water holes appeared at the top of the slope, and the cracks developed in some areas. The central slope is wide about 83 m, the vertical joints develop. Several places on the slope collapsed, and it covered some saplings. There are workers' dormitories, brick factories and a farmhouse at the foot of the landslide. The brick factory is buried extensively by landslide.

The loess usually has great strength and uprightness. It is difficult to form a penetrating structural plane by vertical joints, and the soil is in a basic stable state. In the

long-term rainfall, the soil strength is reduced significantly, the vertical joints will expand rapidly to form transfixion plane in slope. the high-steep slope collapses in the direction of gravity, the slope is instable. After comprehensive analysis, rainfall is a key factor to form a landslide.

### 3.2 Landslide stability calculation

#### 3.2.1 Calculation formula

In this paper, the residual thrust method and finite element method are used to calculate the stability of the landslide in Bailu tableland. The stability of landslide is analyzed quantitatively in Bailu tableland [11]. These methods belong to the rigid limit equilibrium method. The application conditions of rigid limit equilibrium method are as follows: the limit equilibrium state of the failure surface (slip surface) is considered, the deformation and failure of the soil are not considered; the strength of the failure surface (slip surface) is controlled by cohesive force and friction angle ( $c, \varphi$  value), the damage follows the Coulomb criterion; the normal stress and shear stress concentrate on the sliding surface. The slope failure problem is simplified as a plane problem. The following is a detailed introduction of the residual trust method.

The landslide thrust  $E$  is defined as the difference value between the total sliding force ( $\sum T$ ) and the total anti-sliding force ( $\sum R$ ), expressed as  $E = \sum T - \sum R$ . When  $E > 0$ , there is thrust; when  $E < 0$ , there is no thrust; when  $E = 0$ , it is limit equilibrium. The thrust calculation is an indispensable step in slope stability analysis, it is an important basis for landslide control engineering design.

The sliding surface is broken-line sloping surface. The strip is divided according to the undulating condition of the sliding surface. From the trailing edge to the leading edge, the angles between the blocks and the horizontal plane are  $\alpha_1, \alpha_2, \alpha_3, \dots, \alpha_{n-1}, \alpha_n$ , this example only considers the gravity action of the landslide, then the landslide thrust of the  $n$ th block is:

$$E_n = W_n \sin \alpha_n + E_{n-1} \cos(\alpha_{n-1} - \alpha_n) - [W_n \cos \alpha_n f_n + c_n L_n + E_{n-1} \sin(\alpha_{n-1} - \alpha_n) f_n]$$

Where,  $E_n$  is the remaining sliding force of the nth block, it is also named landslide thrust;

$W_n$  is the gravity of the nth block;

$L_n$  is the length of the bottom of the nth block;

$f_n$  is the friction coefficient of the nth block;

$c_n$  is the cohesion of the sliding surface of the nth block.

The formula assumes that the thrust of the nth block is parallel to the slip surface of the n-1th block; similarly, the thrust of the nth block is also parallel to the nth block. (image 3). Actually, the c and  $\phi$  values of each block are not easy to accurately measure, so the anti-sliding force is removed by the safety factor  $F_s$ , it serves as a reserve of strength. The range of  $F_s$  is usually 1.05-1.25. The landslide thrust of the nth block is:

$$E_n = W_n \sin \alpha_n - \frac{1}{F_s} (W_n \cos \alpha_n f_n + c_n L_n) + E_{n-1} \psi_n$$

Where  $\psi_n = \cos(\alpha_{n-1} - \alpha_n) - \frac{1}{F_s} \sin(\alpha_{n-1} - \alpha_n) f_n$ ,  $\psi_n$  is called the transfer coefficient, so the residual thrust method is also called transfer coefficient method.

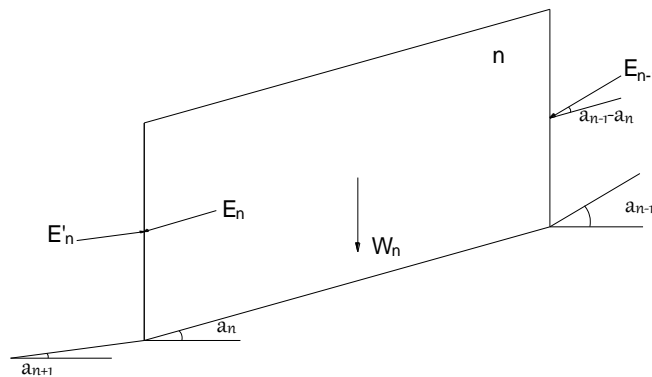


**Figure 3** Force diagram of slider in the nth block



In the calculation process, if  $E_i < 0$ , it indicates that there is no tension between the blocks, so let  $E_i = 0$ . If  $E_i > 0$ , it indicates that the landslide is unstable; if  $E_i < 0$ , it indicates that the landslide is stable; if  $E_i = 0$  it indicates that the landslide is the limit equilibrium state.

### 3.2.2 Calculation Parameter

There is a profile map of the landslide on the north slope of the Bailu tableland (Fig. 4). It is divided by strip. The stability calculation divides the potential landslide profile into six sliders under different moisture contents. The parameters are calculated (Table 2, Table 3).

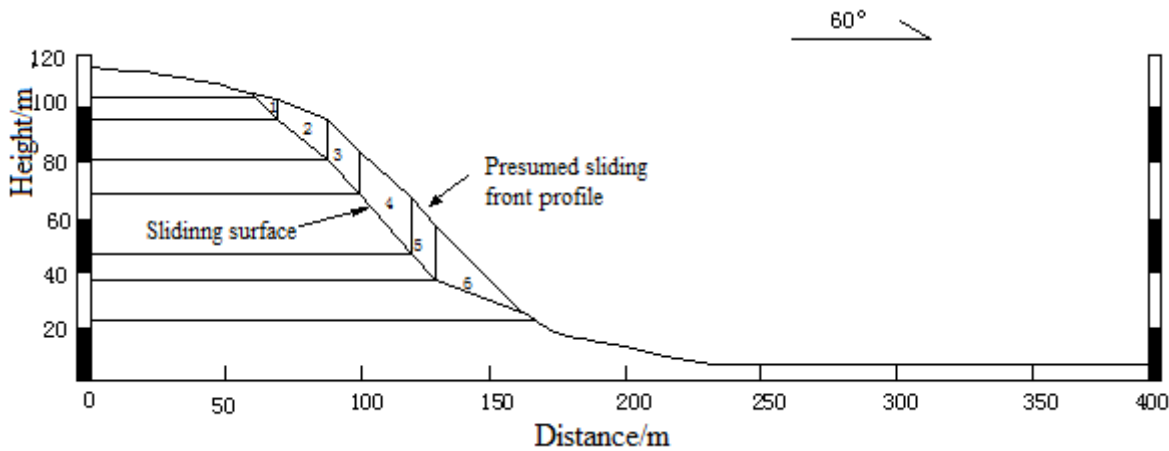


**Figure 4** Block diagram of landslide in northern slope of Bailu tableland

**Table 2** Calculation data for potential stability of the landslide in northern slope of Bailu tableland

Block number	1	2	3	4	5	6
Area/m <sup>2</sup>	36.19	201.89	176.17	341.02	181.91	315.01
Length/m	13.74	23.44	16.95	29.5	13.13	33.94
Inclination/°	45	39	46	49	47	20
Weight of block i Qi/kN	720.18	4017.61	3505.78	6786.29	3620.00	6268.69
Normal component of block i Ni/kN/m	509.24	2528.36	2521.84	5121.68	2647.50	5890.65
Tangential component of block i Ti /kN/m	509.24	2528.36	2521.84	5121.68	2647.50	2144.02

**Table 3** Effective steady-state shear strength indices for different moisture content specimens

Moisture content W/%	Volume moisture content $\theta_m$ /%	Effective cohesion C/KPa	Effective angle of internal friction $\phi$ /°
6	8.22	54.31	26
11	15	27.4	24.8
21	28.77	6.06	23.9
26	35.6	3.51	24.3
30	41.1	3.59	25.2
32	43.84	5.79	24.8

### 3.2.3 The calculation results

the calculation results (the specific gravity is 19.9, the safety factor  $K_s$  is 1.2) are as follows (Fig. 5, Table 4):

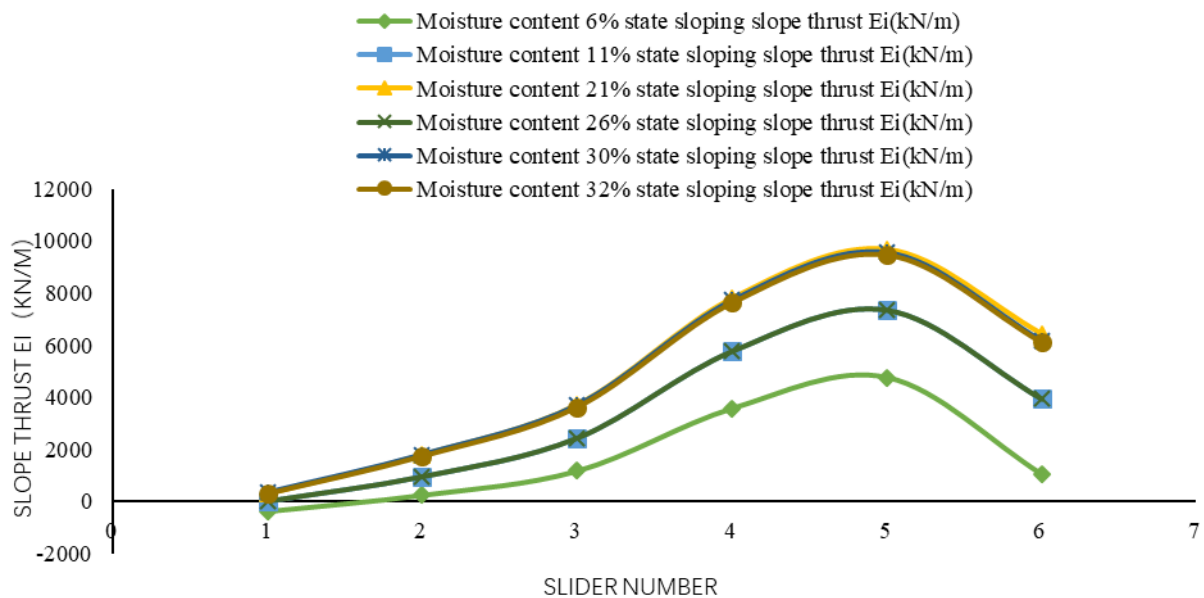


**Figure 5** Broken line diagram of calculation results under different moisture contents

**Table 4** Stability factor under different moisture contents

Moisture content W/%	6	11	21	26	30	32
Stability coefficient Kf	1.15	0.8	0.61	0.6	0.59	0.58

### **3.3 Stability analysis of different moisture contents in northern slope of Bailu tableland**

It can be seen from the calculation results that the shear strength of the soil isn't a complete linear relationship with the moisture content. Some soils are not sensitive to moisture content. The moisture content of the landslide profile is 1.15 in the state of 6% (self-weight). It is in a basically stable state, but partial collapse may occur. The moisture contents are 11%, 21%, 26%, 30% and 32% (self-weight + heavy rain), the corresponding stability coefficients are 0.80, 0.61, 0.6, 0.59, and 0.58. It is in an unstable state, there could be a landslide. The countermeasures should be taken in advance.

## **4 Research on sliding mechanism of "landslide in northern slope of Bailu tableland" based on Phase2**

The main reason for the occurrence of landslide is presistent heavy rainfall. Next is the artificial excavation of slope foot. It rained here for a few days, it is the triggering factor of the landslide. The stability processes of landslide profiles are simulated under different moisture contents, it analyzes the displacement and stress changes of the loess, explore the sliding mechanism of the landslide in northern slope of bailu tableland.

### **4.1 Determine the physical and mechanical parameters of the model**

According to the field survey data, the material soils of the landslide are Q<sub>4</sub>, Q<sub>3</sub>, Q<sub>2</sub> loess and Q<sub>3</sub>, Q<sub>2</sub> paleosol layers. The physical parameters are mainly based on the preliminary test and other engineering related data. The parameters of the soil under different moisture contents are as follows (Table 5, Table 6, Table 7, Table 8, Table 9, Table 10):

**Table 5** Physical and mechanical parameters in natural (6%)

Medium type	Elasticity modulus E/Mpa	Poisson's ratio $\mu$	Saturated compressive strength C/MPa	Internal friction angle $\varphi/^\circ$	Volume-weight KN/m <sup>3</sup>
Q <sub>4</sub>	10	0.45	5	15	15
Q <sub>3</sub>	20	0.35	6.8	23	16.8
Q <sub>2</sub>	25	0.30	7.3	25	18.7
Q <sub>3</sub> Paleosol	23	0.33	7	24	17.5
Q <sub>2</sub> Paleosol	28	0.28	7.5	26	19

**Table 6** Physical and mechanical parameters under moisture content of 11%

Medium type	Elasticity modulus E/Mpa	Poisson's ratio $\mu$	Saturated compressive strength C/MPa	Internal friction angle $\varphi/^\circ$	Volume-weight KN/m <sup>3</sup>
Q <sub>4</sub>	9	0.46	4.9	14	16
Q <sub>3</sub>	17	0.34	6.7	21	16.8
Q <sub>2</sub>	21	0.30	6.9	24	18.7
Q <sub>3</sub> Paleosol	19	0.33	6.9	23	17.9
Q <sub>2</sub> Paleosol	25	0.28	7.5	25	19

**Table 7** Physical and mechanical parameters under moisture content of 21%

Medium type	Elasticity modulus E/Mpa	Poisson's ratio $\mu$	Saturated compressive strength C/MPa	Internal friction angle $\varphi/^\circ$	Volume-weight KN/m <sup>3</sup>
Q <sub>4</sub>	16	0.46	4.7	12	17
Q <sub>3</sub>	11	0.37	6.6	18	16.9
Q <sub>2</sub>	29	0.31	6.8	23	18.8
Q <sub>3</sub> Paleosol	13	0.34	6.8	22	18.1
Q <sub>2</sub> Paleosol	17	0.29	7.4	24	19.1

**Table 8** Physical and mechanical parameters under moisture content of 26%

Medium type	Elasticity modulus E/Mpa	Poisson's ratio $\mu$	Saturated compressive strength C/MPa	Internal friction angle $\varphi/^\circ$	Volume-weight KN/m <sup>3</sup>
Q <sub>4</sub>	12	0.47	4.6	11	18
Q <sub>3</sub>	9	0.38	6.6	16	17
Q <sub>2</sub>	6	0.32	6.7	22	19
Q <sub>3</sub> Paleosol	10	0.35	7.4	24	18.3

Q <sub>2</sub> Paleosol	14	0.30	7.3	21	19.2
-------------------------	----	------	-----	----	------

**Table 9** Physical and mechanical parameters under moisture content of 30%

Medium type	Elasticity modulus E/Mpa	Poisson's ratio $\mu$	Saturated compressive strength C/MPa	Internal friction angle $\varphi/^\circ$	Volume-weight KN/m <sup>3</sup>
Q <sub>4</sub>	5	0.5	4.5	10	15
Q <sub>3</sub>	6	0.4	6.5	15	17
Q <sub>2</sub>	9	0.32	7.0	22	19
Q <sub>3</sub> Paleosol	7	0.35	6.7	20	18
Q <sub>2</sub> Paleosol	10	0.3	7.3	23	19.2

**Table 10** Physical and mechanical parameters under moisture content of 32%

Medium type	Elasticity modulus E/Mpa	Poisson's ratio $\mu$	Saturated compressive strength C/MPa	Internal friction angle $\varphi/^\circ$	Volume-weight KN/m <sup>3</sup>
Q <sub>4</sub>	5	0.56	4.5	10	19
Q <sub>3</sub>	7	0.39	6.5	15	17
Q <sub>2</sub>	10	0.32	6.7	21	19
Q <sub>3</sub> Paleosol	8	0.35	7	20	18.3
Q <sub>2</sub> Paleosol	11	0.3	7.3	22	19.2

#### 4.2 Model

The profile established by CAD is imported into Phase2, the two-dimensional finite element model is established and meshed. The model is divided into triangles by finite element unit division. The length is 251m, the height is 155m. Constraint: The upper part of the model is a natural horizontal plane, the applied load on the ground is regardless, there is no constraint on the upper part of the model; the horizontal displacement is constrained by the left and right boundaries; the bottom boundary is fixed.

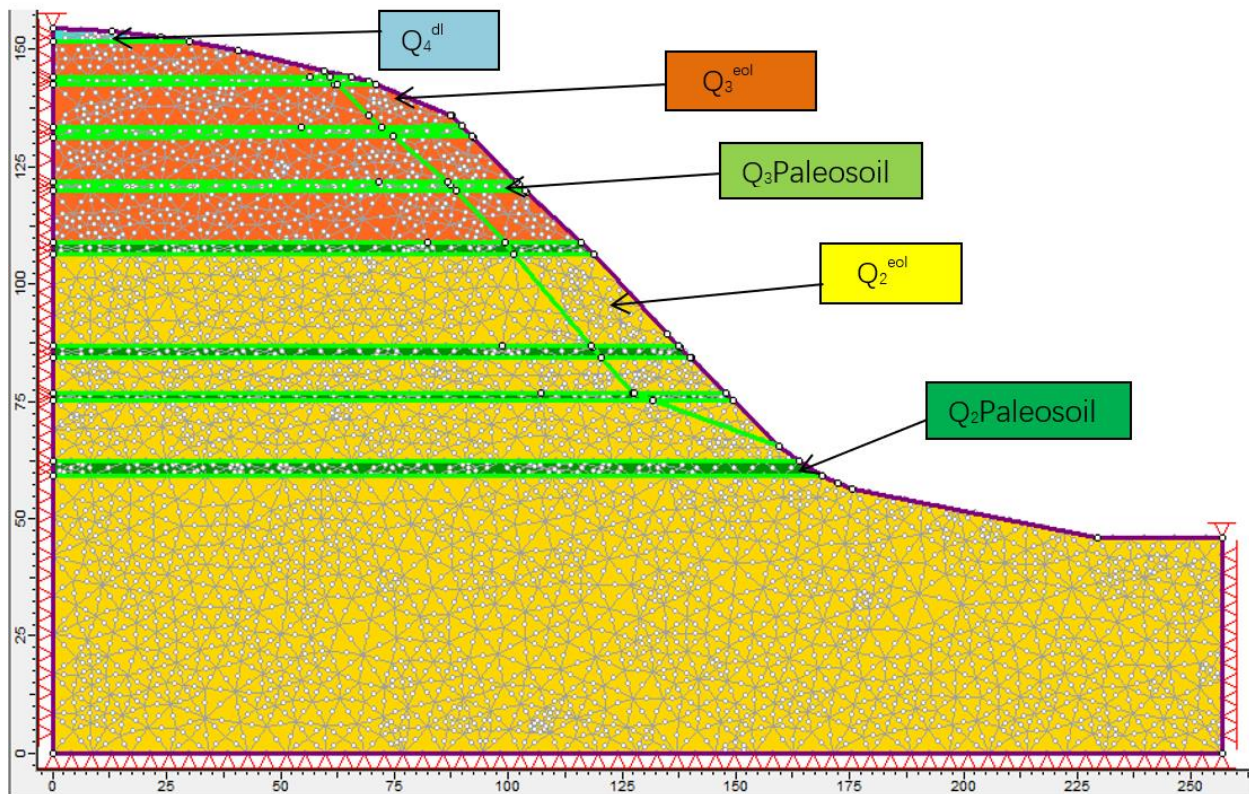
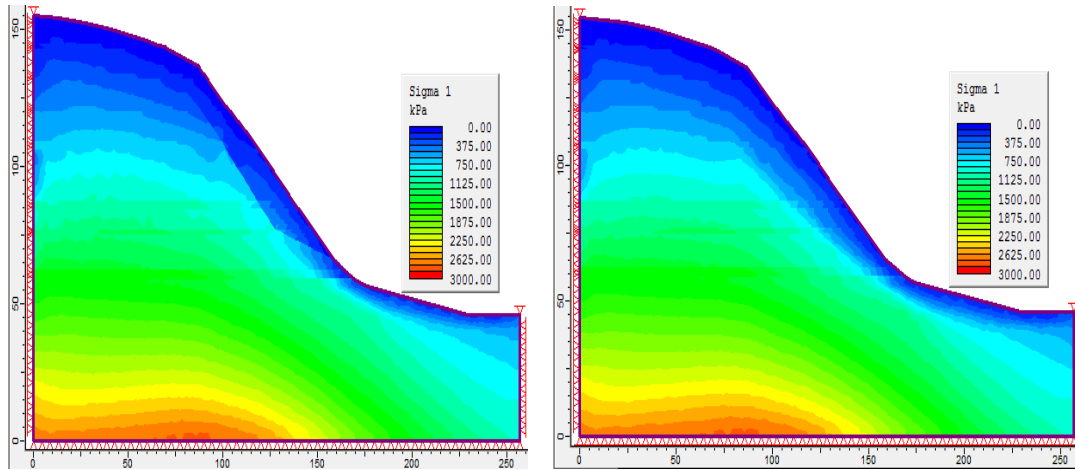


**Figure 6** Calculation model of landslide in northern slop of Bailu tableland

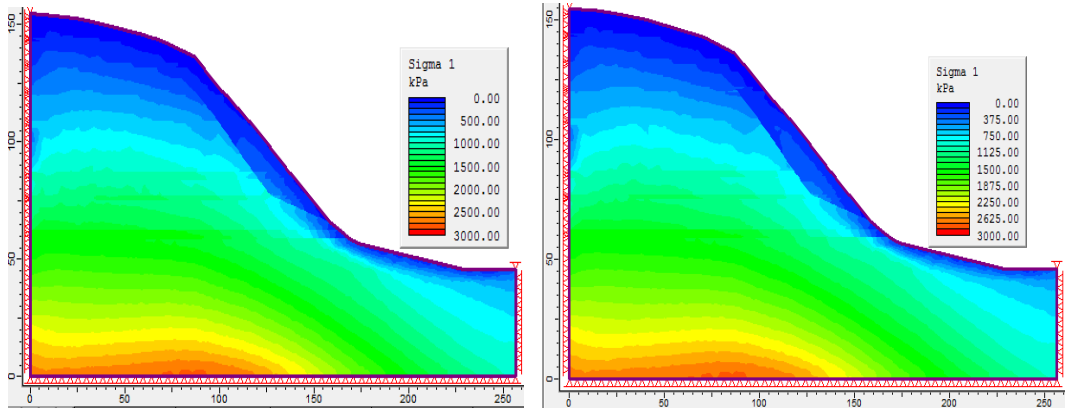
### 4.3 Simulation results and analysis

Six groups of soil with different moisture content are simulated numerically to calculate the slope stability. The physical and mechanical parameters are assigned to the soil above the slip surface, the principal stress distribution of the landslide is simulated under different moisture contents (Fig. 7):



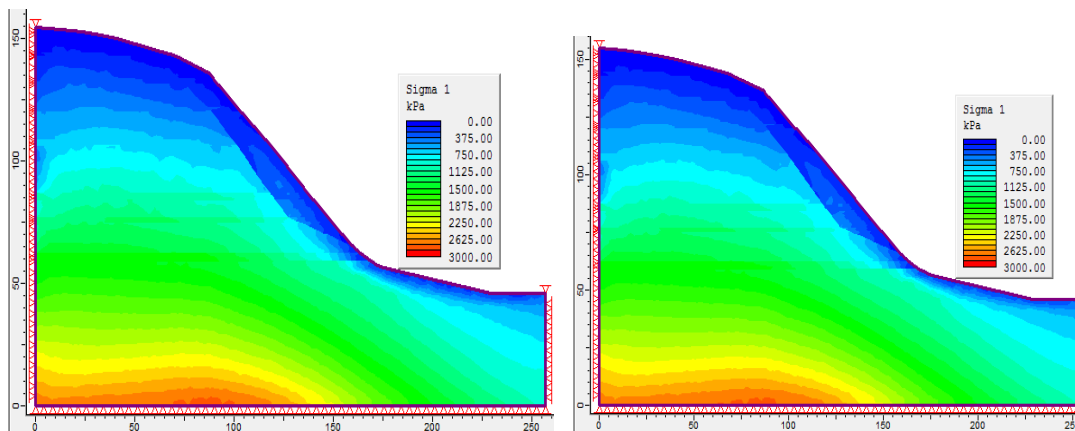
a Distributi on of principal stress (6%)

b Distributi on of principal stress(11%)



c Distributi on of principal stress (21%)

d Distributi on of principal stress(26%)



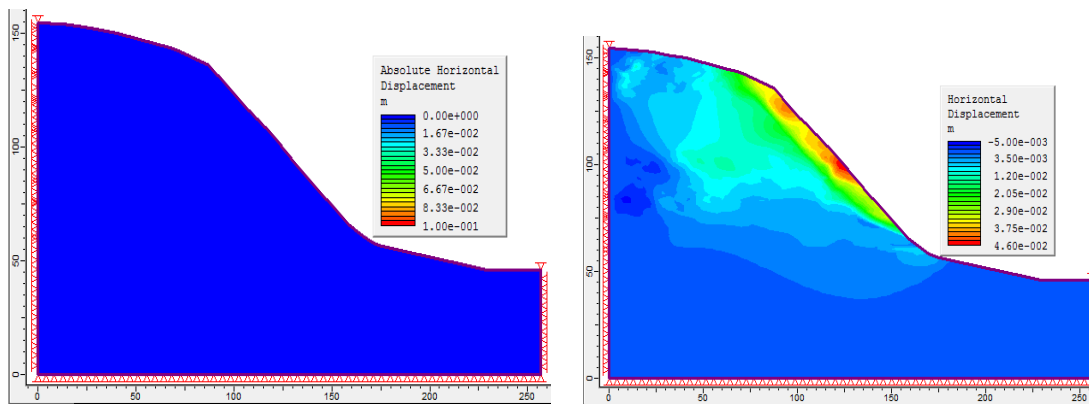
e Distributi on of principal stress (30%)

f Distributi on of principal stress(32%)

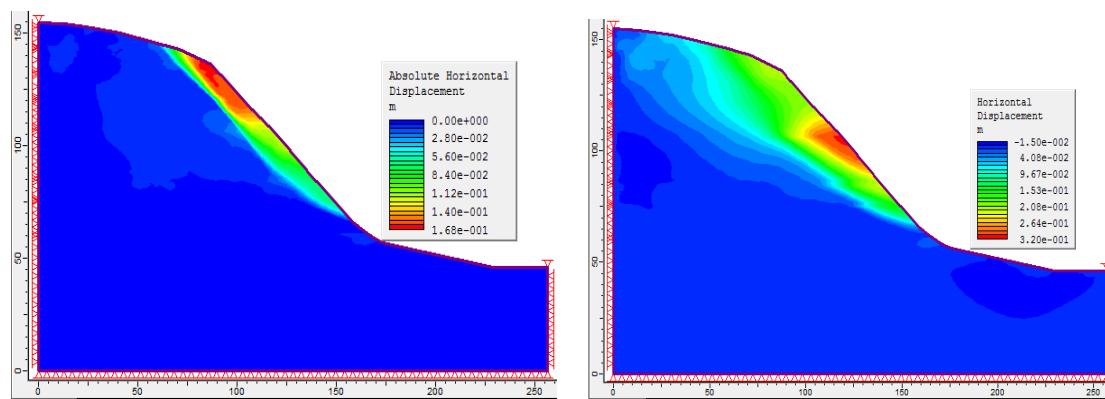
**Figure 7** Distribution of principal stress under different moisture contents

The figures show the magnitude of the principal stress in different colors, and the color from light to dark indicates that the principal stress gradually increases. It can be seen from the figure that the principal stress increases with increasing depth. As the moisture content increases, the principal stress of the soil above the slip surface also increases.

Six groups of soil with different moisture content are simulated numerically to calculate the slope stability. The physical and mechanical parameters are assigned to the soil above the slip surface, the horizontal displacement distribution of the landslide is simulated under different moisture contents (Fig. 8):

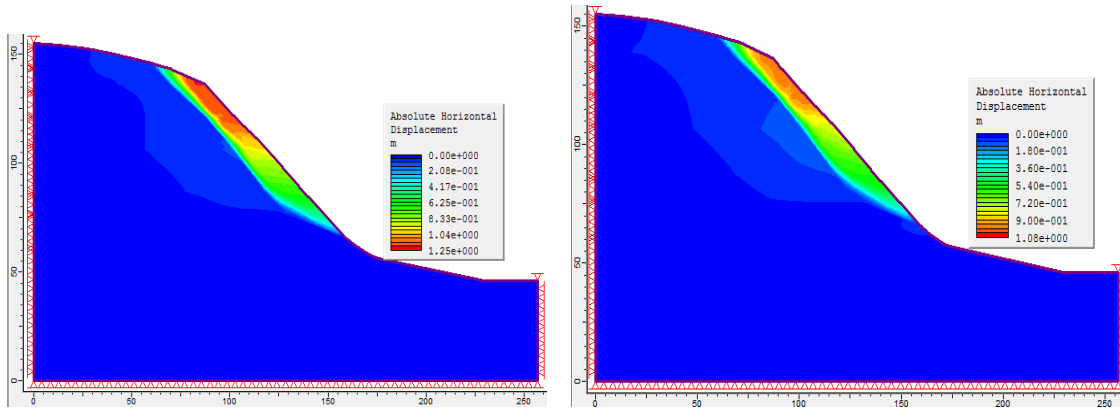


a Distributi on of horizontal displacement (6%) b Distributi on of horizontal displacements(11%)



c Distributi on of horizontal displacement (21%) d Distributi on of horizontal displacements(26%)



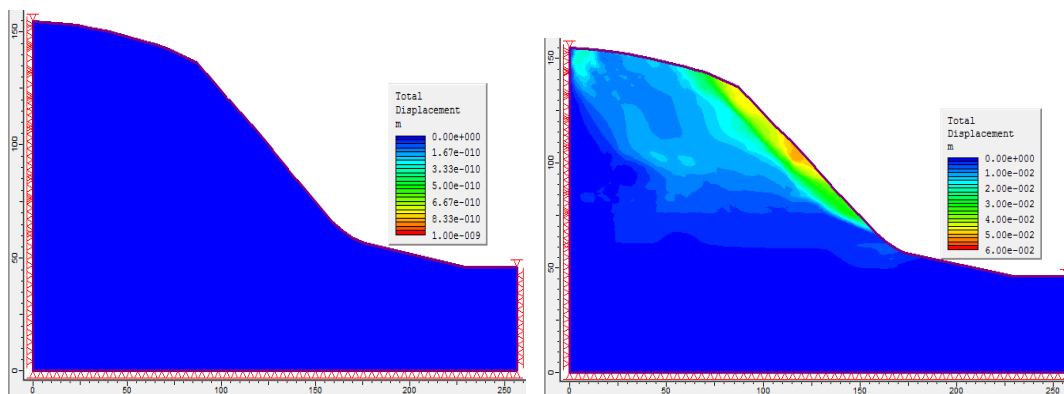


e Distributi on of horizontal displacement (30%) f Distributi on of horizontal displacements(32%)

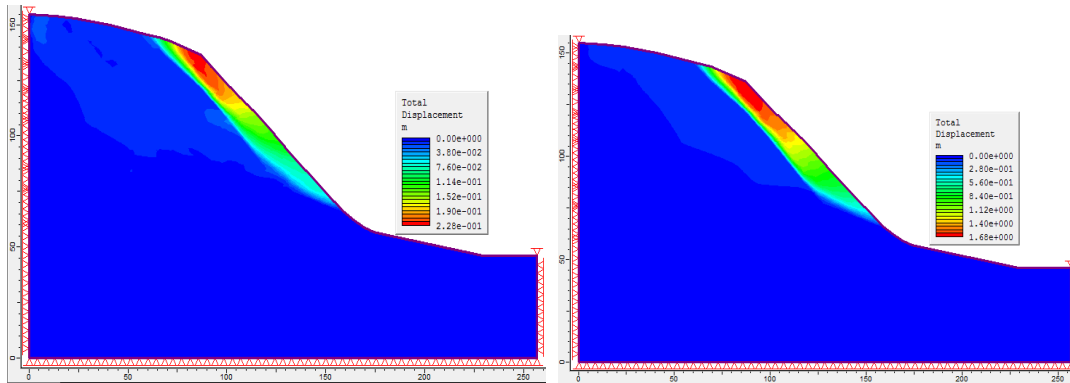
**Figure 8** Horizontal displacement under different moisture contents

The figures show that the horizontal displacement of the soil above the slip surface increases with the moisture content increases. Under the natural (6%) moisture content, it is in stability. When the water content is 11%, the maximum horizontal displacement is 0.046m, When the water content is 32%, the horizontal maximum displacement is 1.25m.

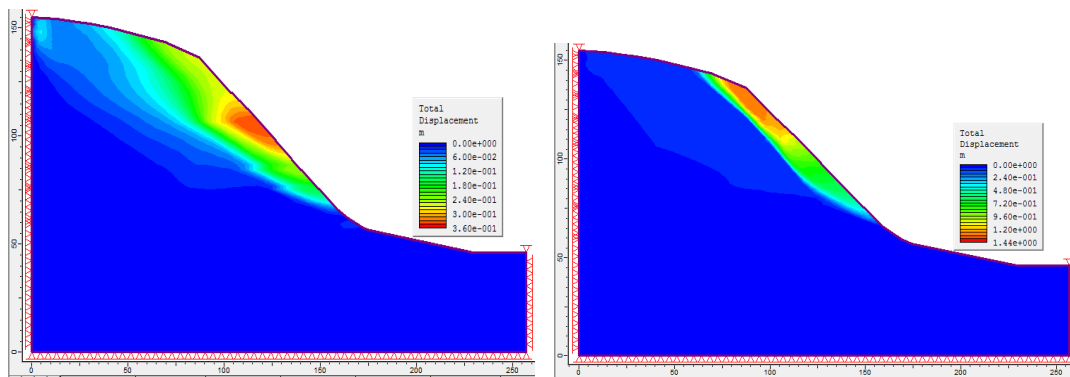
Six groups of soil with different moisture content are simulated numerically to calculate the slope stability. The physical and mechanical parameters are assigned to the soil above the slip surface, the total displacement distribution of the landslide is simulated under different moisture contents (Fig. 9):



a Distributi on of total displacement (6%) b Distributi on of total displacements(11%)



c Distribution of total displacement (21%) d Distribution of total displacements(26%)



e Distribution of total displacement (30%) f Distribution of total displacements(32%)

**Figure 9** Distribution of total displacement under different moisture contents

The figures show that the total displacement of the soil above the slip surface increases with the moisture content increases. Under the natural (6%) moisture content, it is in stability. When the water content is 11%, the maximum total displacement is 0.055m, When the water content is 32%, the total maximum displacement is 1.44m.

#### 4.4 Conclusion

It is studied that the stability of the landslide in northern slope of bailu tableland under different moisture content. the stress and displacement are simulated under different moisture. The simulation results are analyzed, the slope is in a stable state under the natural condition; as the moisture content increases, it becomes more unstable. Compared with the calculation results of the transmission force system method, the simulation results

of the model are consistent with the actual situation. It is our expected result, which finally shows the rationality of the simulation.

## 5 Advice

The prevention of landslide disasters is an important project, the principle is that put prevention first and combine prevention with treatment. Landslides occur frequently, it causes serious damage. Most of them are in rural areas, landslide prevention has been neglected largely. In order to ensure the production facilities and personal safety in the area, it is necessary to prevent landslides and disasters. According to the local situation, it believes that drainage engineering, slope cutting engineering and biological measures can be considered to control the source landslide comprehensively.

## References:

- [1] EW. Brand. Landslides in Hong Kong during the Rainfall Ewent. *Landslide News*. No. Aug 8,1994.
- [2] R K. Mark,E B. Newman. Rainfall totals before and during the storm: distribution and correlation with damaging landslides [A].
- [3] Li Chaofen, Chen Hong. Rainwater infiltration and landslide disaster in Hong Kong. *Hydrogeological engineering geology*, 1997,04:36-40.
- [4] Li Changjiang, Ma Tuhua, Sun Leling, et al. A new method for calculating the effective rainfall in the early stage of rainfall landslide prediction, *Mountain Journal*, 2011, 01: 81-86.
- [5] Successful prediction of landslides in the Heifangtai area of Gansu. *China Geological Survey*, edited, No. 13
- [6] Sun Weiqing. Study on mechanical response mechanism of excavation unloading loess landslide. Chang'an University, 2013.
- [7] Xian Urban Planning Administration, Xi'an Survey and Mapping Institute. *Xi'an Urban Engineering Geology Atlas*. Xi'an: Xi'an Map Press, 1998.
- [8] Wang Qingyu, Pei Xianzhi. Analysis of Structural Characteristics of the Weihe Rift Basin. *Journal of Xi'an Institute of Geology*, 1990, (1).
- [9] Shanxi Provincial Bureau of Geology and Mineral Resources. *Regional Geology of Shaanxi Province*. Beijing: Geological Publishing House, 1989.
- [10] Shanxi Provincial Bureau of Geology and Minerals. *Shaanxi Province Geology*. Beijing: Geological Publishing House, 1983.
- [11] Zhang Yuyuan, Wang Shitian, Wang Lansheng, *Principles of Engineering Geology Analysis (Second Edition)*, Beijing: Geological Publishing House, 1994.3.

This paper DOI: [10.5281/zenodo.2995977](https://doi.org/10.5281/zenodo.2995977)



**Journal Website: <http://ijgsw.comze.com/>  
You can submit your paper to email: [Jichao@email.com](mailto:Jichao@email.com)  
Or [IJGSW@mail.com](mailto:IJGSW@mail.com)**